

# Computational Study of Transition of Oil-water Flow Morphology due to Sudden Contraction in Microfluidic Channel

J. Chaudhuri<sup>1</sup>, S. Timung<sup>1</sup>, T. K. Mandal<sup>1,2</sup>, and D. Bandyopadhyay <sup>\*1,2</sup>

<sup>1</sup>Department of Chemical Engineering, Indian Institute of Technology Guwahati, India.

<sup>2</sup>Centre for Nanotechnology, Indian Institute of Technology Guwahati, India.

\*Corresponding Author: Department of Chemical Engineering, Indian Institute of Technology Guwahati, India,  
Pin – 781039, Email: [dipban@iitg.ernet.in](mailto:dipban@iitg.ernet.in)

**Abstract:** The present study shows a strategy to transform larger two-phase flow structures into the smaller ones by incorporating simple tuning of microchannel geometry. The two-phase flow is modelled employing the in-built phase-field model which is commercially available with COMSOL Multiphysics software. With the help of a series of numerical simulations, we show that larger plug flow can be transformed into smaller droplets by introducing an orifice at the T-junction of the microfluidic channel. The size of the droplets can be tuned by varying the diameter of the orifice. In addition, the frequency of droplets can also be varied by changing the diameter and position of the orifice along the length of the microfluidic channel. The results shown in this study can be helpful in the design of micro-emulsifiers and microreactors which demands a collection of miniaturized droplets dispersed inside a continuous medium.

**Keywords:** multiphase flow; microfluidic channel; computational fluid dynamics; mixing.

## 1. Introduction

The control over the flow morphologies of two-phase flow inside microfluidic devices have been a subject

of interest for the past few decades because they can be applied to a wide range of applications in various fields of science and technology [1-4]. The microscopic technologies offer several advantages over the conventional macroscopic ones because of the availability of higher surface to volume ratio, ability to handle small volume of fluids, easier process control and reduction in operating cost [5]. While the effect of gravity and inertial forces become weaker with reduction in channel diameter, the influence of surface and viscous forces becomes stronger. However, very often the flow structures such as slug and plug flow are encountered [6,7], which are not that desirable for the processes where higher surface to volume ratio is in demand. Thus, it is of importance to identify the conditions for developing smaller size flow structures where higher surface to volume ratio can be easily achieved.

In this direction, various strategies have been explored to control the two-phase flow morphologies and their transitions from slug to plug to droplet, with the variation in the different process parameters. Previous studies reveal that the flow morphologies can be controlled by varying the velocity of fluids [8], fluid properties such as interfacial tension [9] and viscosity [10], and wettability of the fluid on the wall.

For example, flow transition from droplet to slug to annular flow can be achieved by increasing the flow rate of disperse phase whereas larger slugs are transformed into smaller droplets by increasing the viscosity of the continuous phase. A very recent study [9] shows that water-in-oil and oil-in-water emulsion can also be prepared in a single microfluidic channel by introducing surfactants at specific concentrations in the oil and water phases. Further, another study [7] show the transformation of the flow morphologies from steady to unsteady when the diameter of the microchannel is less than 250  $\mu\text{m}$ . In the present work, we study the transition of flow patterns due to marginal change in channel geometry. This is accomplished by placing an orifice at the T-junction, which creates an abrupt contraction and expansion inside the microfluidic channel. With the help of series of 2D simulations, we show that by introducing an orifice near the microchannel T-junction, the larger flow structures can easily be transformed into smaller droplets, which can be employed to develop droplet driven flows.

## 2. Use of COMSOL Multiphysics

In order to model the oil-water flow inside the microchannel, we use the laminar and incompressible two-phase flow setup with the phase-field model to track the interface in the commercially available COMSOL Multiphysics software.

### 2.1 Problem Formulation

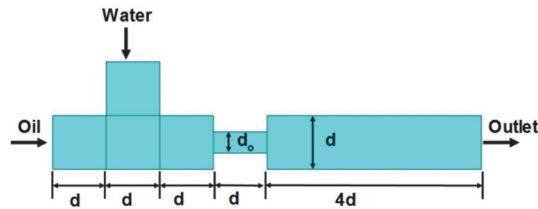


**Figure 1.** Geometry of the microchannel.

Figure 1 schematically shows the geometry under consideration. Here the channel diameter,  $d = 500 \mu\text{m}$ , and diameter of constriction,  $d_o = 500, 200, 150$  and  $100 \mu\text{m}$ . Oil (water) flows in the microchannel through horizontal (vertical inlets) and flows out through the outlet as shown by the direction of arrows. The flow of a pair of incompressible, immiscible and Newtonian fluids inside a T-shaped microchannel are governed by the following continuity and equations of motion,

$$\nabla \cdot \mathbf{u}_i = 0, \quad (1)$$

$$\rho(\dot{\mathbf{u}}_i + \mathbf{u}_i \cdot \nabla \mathbf{u}_i) = -\nabla p_i + \nabla \cdot \boldsymbol{\tau}_i + \mathbf{f}_{st} + \rho \mathbf{g} \quad (2)$$

In the Eqs. (1) and (2) the subscript ' $i$ ' corresponds to oil ( $i = 1$ ) and water ( $i = 2$ ) phases. The notations,  $\mathbf{u}_i$  denotes the velocity vector,  $\eta_i$  is dynamic viscosity,  $\rho_i$  is density,  $p_i$  is the pressure of the  $i^{\text{th}}$  fluid. The over dot denotes the time derivative and the vector  $\mathbf{g}$  is the acceleration due to gravity acting on the negative  $y$  direction for the geometry shown in the Figure 1. The constitutive relation for the  $i^{\text{th}}$  Newtonian fluid is considered as,

$$\boldsymbol{\tau}_i = \eta_i (\nabla \mathbf{u}_i + \nabla \mathbf{u}_i^T).$$

We employed phase field computational method to track the interface. The transport equation for this phase field parameter ( $\phi$ ) is,

$$\dot{\phi} + \mathbf{u}_i \cdot \nabla \phi = \nabla \cdot \chi (\nabla G) \quad (3)$$

The parameter  $\phi$  is  $-1$  for water and  $1$  for oil. The variable  $\chi$  represent the mobility of the interface and the chemical potential is defined as,  $G = F'(\phi) = \lambda [-\nabla^2 \phi + \phi(\phi^2 - 1)/N^2]$ . The chemical potential is evaluated as,

$$F(\phi) = \int_V f_{tot} dV = \int_V \left( f(\phi) + \frac{1}{2} \lambda |\nabla^2 \phi| \right) dV \quad (4)$$

In Eq. (4),  $f_{tot}$  is the total free energy density, which is the sum of the bulk energy or double well potential [ $f(\phi) = \lambda / 4N^2 (\phi^2 - 1)^2$ ] and the surface energy. The mixing energy density is expressed as,  $\lambda = (3\gamma N) / (2\sqrt{2})$ , in which  $\gamma$  and  $N$  are the interfacial tension and thickness of the diffused interface. The interfacial density, viscosity, permittivity, and conductivity, are evaluated in terms of  $\phi$  as,  $\rho = 0.5 [\rho_1(1+\phi) + \rho_2(1-\phi)]$  and  $\eta = 0.5 [\eta_1(1+\phi) + \eta_2(1-\phi)]$ . The surface tension force in Eq. (2) is defined as a product of the chemical potential  $G$  and the gradient of the phase field ( $\phi$ ) as,

$$\mathbf{f}_{st} = G \nabla \phi. \quad (5)$$

## 2.2 Boundary conditions

Figure 1 schematically shows the geometry of the problem considered. At the inlets, normal inflow velocity ( $\mathbf{v}_i = U$ ) boundary condition and at the outlet, default pressure with no viscous stress boundary condition are enforced. The walls are wetting, non-slipping, and impermeable. The equilibrium contact angle ( $\theta$ ) of a water droplet on the wall and embedded inside oil is set to  $140^\circ$ . The "physics-controlled" meshing scheme was chosen with "fine" element size, which created triangular cells with almost 7000 cells inside the control volume. Silicone oil and water were chosen as the test fluids. The densities of oil and water phase were kept at  $1000 \text{ kg/m}^3$ . The viscosities of oil and water phase were kept at  $0.01$  and  $0.001 \text{ Pa s}$ , respectively. The

interfacial tension  $\gamma$  between oil and water phases were varied from  $0.04 - 0.0258 \text{ N/m}$ .

## 3. Results and discussions

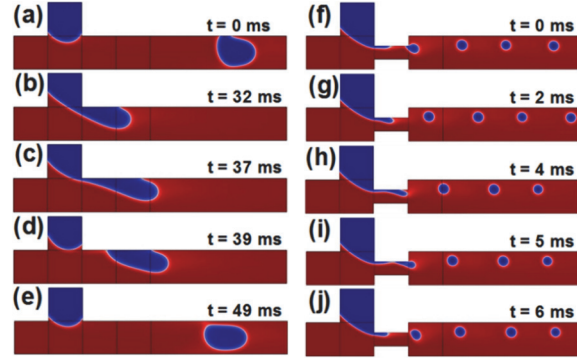


**Figure 2.** Full cycle of the formation of oil-water flow structures in a T-junction microchannel without and with an orifice. Images (a) – (e) show the mechanism of plug formation at different time ( $t$ ) interval in millisecond (ms). While images (f) – (j) show the mechanism of formation of flow structure in presence of an orifice at different time interval.

The images (a) – (e) in the Figure 2 shows the formation of a water plug (darker blue shade) in continuous oil phase (lighter red shade), which is commonly observed in the two-phase flow studies<sup>7, 8</sup>. In this case, the velocity of oil ( $U_o$ ) and water ( $U_w$ ) are taken to be  $0.1$  and  $0.01 \text{ m/s}$ , respectively. The subscript  $o$  and  $w$  represents oil and water phases. Figure 2 (f) – (j) shows the pathway of droplet formation for a similar flow condition in presence of sudden contraction inside the microfluidic channel. Clearly, the figure suggests that the flow is transformed from plug to droplets with increased droplet frequency, due to the presence of an orifice. The channel contraction at the T-junction induces an abrupt velocity difference in the oil and water phases, which cause higher shear at the oil-water interface at the zone of contraction. In consequence, the water

phase penetrating into the oil in this region produces smaller droplets

Further, the diameter of orifice,  $d_o$  and the interfacial tension ( $\gamma$ ) are found to have a strong influence on the droplet diameter,  $d_d$ , which is depicted in Figure 3 (a) – (d) in which  $d_o$  is set to 200, 150 and 100  $\mu\text{m}$  in images (b), (c) and (d), respectively. Figure 3 (e)

shows the variation of dimensionless droplet diameter,  $h_d$  ( $= d_d/d$ ) with dimensionless orifice diameter,  $h_o$  ( $= d_o/d$ ) at different interfacial tension  $\gamma$ . These plots suggest that wide range of droplet diameter could be achieved by controlling orifice diameter and  $\gamma$ .

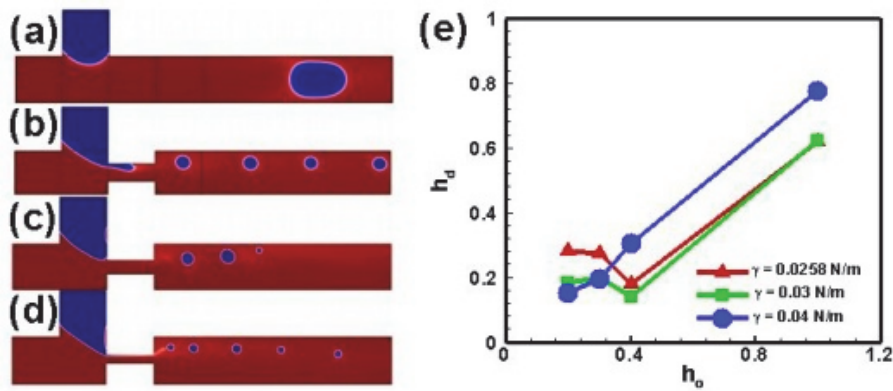


**Figure 3.** Flow transition from large size plug to minute droplets due to presence of orifice at the T junction. Here, from (a) – (d), the diameter of orifice,  $d_o$  decreases from 0.5 – 0.1 mm such that the value of dimensionless orifice diameter,  $h_o$  ( $= d_o/d$ ) = 1, 0.4, 0.3, and 0.2, respectively. Image (e) shows the variation of dimensionless droplet diameter,  $h_d$  ( $= d_d/d$ ) with  $h_o$  at different values of  $\gamma$ .

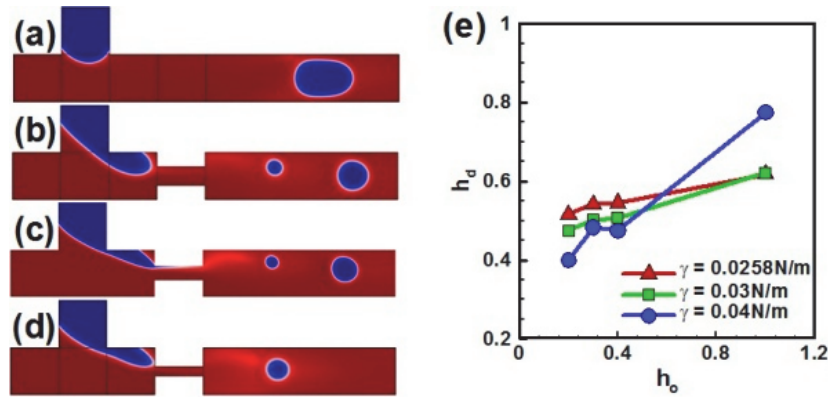


**Figure 4.** Flow transition from large size plug to smaller droplets due to presence of orifice at a distance  $d$  from T-junction. Here, from (a) – (d), the diameter of orifice,  $d_o$  decreases from 0.5 – 0.1 mm such that the value of dimensionless orifice diameter,  $h_o$  ( $= d_o/d$ ) = 1, 0.4, 0.3, and 0.2, respectively. Image (e) shows the variation of dimensionless droplet diameter,  $h_d$  ( $= d_d/d$ ) with  $h_o$  at different values of  $\gamma$ .

The position of the orifice ( $d$ ) from the T-junction is also found to have a significant influence on the flow morphology. Plots (a) – (d) in Figure 4 show a transition of flow morphology from plug to droplets in such cases. Further the figure shows that in these situations also  $d_o$  decreases with  $d_d$ , as observed for the previous figure. Figure 4 (e) shows the dependence of dimensionless droplet diameter,  $h_d$  with dimensionless orifice diameter,  $h_o$  at various values of  $\gamma$ . The plot shows that the flow in smaller orifice diameter could develop smaller size droplets.

#### 4. Conclusions

The present study shows a simple strategy to control the oil-water flow patterns by placing a abrupt contraction near a T-junction of a microchannel. The results revealed that smaller diameter orifice could facilitate smaller size flow structures. Also the frequency and size of droplet could be well control by the size of orifices and their positions. This approach can be well utilized in microfluidic devices where flow structures with high surface to volume ratio are desired.

#### 5. Acknowledgement

The authors are thankful to Department of Chemical Engineering, Indian Institute of Technology Guwahati for providing facilities and support to carry out this research.

#### 6. References

1. S. W. Li, J. H. Xu , J. Tan , Y. J. Wang , G. S. Luo Controllable Preparation of Monodisperse O/W and W/O Emulsions in the Same Microfluidic Device, *Langmuir*, **22**, 7943 (2006).
2. C.-X. Zhao, L. He, S. Z. Qiao, and A. P. J. Middelberg, Nanoparticle synthesis in microreactors, *Chemical Engineering Science*, **66**, 1463 (2011).
3. X. Z. Lin, A. D. Terepka, and H. Yang, Synthesis of Silver Nanoparticles in a Continuous Flow Tubular Microreactor, *Nano Letters*, **4**, 2227 (2004).
4. J. Skommer, J. Akagi, K. Takeda, Y. Fujimura, K. Khoshmanesh, and D. Wlodkowic, Multiparameter lab-on-a-chip flow cytometry of the cell cycle, *Biosensors and Bioelectronics*, **42**, 586 (2013).
5. V. Kumar, M. Paraschivou, and K. D. P. Nigam, Single-phase fluid flow and mixing in microchannels, *Chemical Engineering Science*, **66**, 1329 (2011).
6. A. Kawahara, P. M. Y. Chung, and M. Kawaji, Investigation of two-phase flow pattern, void fraction and pressure drop in a microchannel, *International Journal of Multiphase Flow*, **28**, 1411 (2002).
7. P. M. Y. Chung and M. Kawaji, The effect of channel diameter on adiabatic two-phase flow characteristics in microchannels, *International Journal of Multiphase Flow*, **30**, 735 (2004).
8. H. Foroughi and M. Kawaji, Viscous oil–water flows in a microchannel initially saturated with oil: flow patterns and pressure drop characteristics, *International Journal of Multiphase Flow*, **37**, 1147 (2011).
9. J. H. Xu, S. W. Li, J. Tan, Y. J. Wang, and G. S. Luo, Controllable Preparation of Monodisperse O/W and W/O Emulsions in the Same Microfluidic Device, *Langmuir*, **22**, 7943 (2006).
10. T. Cubaud, B. M. Jose, S. Darvishi, and R. Sun, Droplet breakup and viscosity-stratified flows in microchannels, *International Journal of Multiphase Flow*, **39**, 29 (2012).